Strongly Stretched Semiflexible Extensible Polyelectrolytes and DNA

Roland R. Netz

Max-Planck-Institut für Kolloid und Grenzflächenforschung, Am Mühlenberg, 14424 Potsdam, Germany

Received April 2, 2001; Revised Manuscript Received July 18, 2001

ABSTRACT: The stretching response of a single charged semiflexible and extensible polymer in the limit of large tensile forces is calculated. We consider the effects of (i) the coupling of bending and elongational fluctuations, (ii) the electrostatic contribution to the bending and elongational energies, and (iii) nonlinear bare elastic elongational energies. We show that the electrostatic repulsion between charged monomers leads to an intrinsic stretching force, which cannot be neglected for low salt concentrations. For DNA this effect shifts the B-DNA−S-DNA transition to lower external forces as the salt concentration is decreased, in agreement with experiments. Because of the scale dependence of the electrostatic contribution to the persistence length, the effective persistence length (obtained from fitting the high-force stretching response to a semiflexible chain model) acquires a force dependence which follows a universal heuristic scaling function. As a consequence, flexible (synthetic) polyelectrolytes are characterized by their bare persistence length in the piconewton force range, while the effective persistence length of double-stranded DNA contains additional electrostatic contributions in the same force range as was found in recent experiments. The coupling between elongational and bending fluctuations leads to a force renormalization which is particularly important close to conformational phase transitions or bond failure. Finally, these perturbative results are supplemented by quantum-chemical ab initio calculations for the stretching response of polymers, giving an elastic modulus of 28 nN for fully saturated carbon-backbone polymers (plus nonlinear corrections which are dominant close to bond failure).

Introduction

Since the advent of single-molecule manipulation techniques, large amounts of experimental data have been accumulated on the response of polymers to stretching forces.[1] Using magnetic beads, the extension of single DNA molecules has been determined in the force range of 100 fN to 10 pN[2] and found to be well described by the semiflexible chain model.[3−7] Atomic force microscopy allows forces to be measured in the range from 10 pN up to covalent-bond breakage at a few nanonewtons and has been used to study DNA,[8] proteins,[9] polysaccharides,[10] synthetic neutral polymers,[11] and synthetic polyelectrolytes.[12,13] Yet another method involves using a membrane capsule as force transducer with a sensitivity from 10 fN to several nanonewtons.[14] For forces of about 10 pN the elastic elongation of the polymer contour length becomes important and has to be included in the theory.[5,15] For charged chains, the stretching behavior is influenced by the presence of charges on the polymer backbone. Barrat and Joanny showed that the electrostatic contribution to the chain stiffness, described by the electrostatic contribution to the persistence length, l_{OSF},[16−18] depends on the scale of the bending fluctuations,[19] leading to a softening of the charged chain for bending wavelengths smaller than the screening length. For stretching under applied force, this means that the effective bending stiffness decreases for large forces and as the salt concentration is increased, as has been predicted theoretically and verified by experiments.[6] However, a few experimental points remained unclear: (i) In experiments in the large force range of stretched DNA, it was found that decreasing the salt concentration makes the chain stiffer with respect to bending fluctuations but softer with respect to elongational fluctuations, in direct contradiction with linear elasticity theory.[20] (ii) One of the salient experimental results is that DNA is, at forces of 10 pN, described by a semiflexible chain with a persistence length of about 50 nm, which corresponds to the sum of bare and electrostatic persistence length,[21] while synthetic polyelectrolytes are, for the same force, described by a persistence length corresponding to the bare persistence length alone,[12,13] which is of the order of 1 nm. (iii) Finally, the transition from B-DNA to S-DNA, which happens at high salt concentrations at a force of roughly 65 pN and involves a conformational change of the molecular structure of DNA and a length increase by a factor of 1.7,[22,23] shifts to lower forces as the salt concentration is increased[20,23,24] or the pH is changed from its normal value.[25]

In this paper we describe a theory that includes the coupling of elongational and bending fluctuations, nonlinear contributions to the bare elastic elongational energy, and the effects of electrostatic interactions of polyelectrolytes under tensile forces. The stretching force is assumed to be large, such that the polymer is predominantly aligned parallel to the applied force. The mechanical response of the polymer backbone to elongation is described by an arbitrary local energy function and thus can be chosen to include nonlinear elasticity and conformational changes of the polymer at large stretching forces. The coupling of elongational and bending fluctuations leads to a renormalization of the effective force: elongation and bending contributions to the total extension are not additive, in contrast to the formulas that are commonly used to fit experimental data. The charges along the chain lead to an increased stiffness of the chain with respect to bending modes; they also lead to an intrinsic stretching force which pushes the monomers apart. This effect turns out to be quite important at low salt concentrations and can quantitatively account for the fact that the B-DNA−S-DNA transition shifts to lower external forces as the salt concentration is decreased.[20] The electrostatic

10.1021/ma010555u CCC: $20.00
Published on Web 09/11/2001

contribution to the bending rigidity is scale dependent. The effect of the softening of the chain at large tensile forces can be described by a universal scaling function, which holds to a very good approximation for all different salt concentrations and bare bending stiffnesses. Here we find that polymers with a small bare persistence length (that is all synthetic polymers with a nonconjugated carbon backbone) are in the piconewton range and for intermediate salt concentration characterized by their bare bending rigidity, while stiff molecules (such as DNA) are in the same force range and under similar salt conditions characterized by the sum of the bare and the electrostatic persistence lengths. This finding is in quantitative agreement with experiments on synthetic polymers[12,13] and DNA.[2,6,15] Finally, we also performed ab initio quantum-chemical calculations and determined the full nonlinear elongational elastic energy of a set of alkane molecules of different lengths. We obtain the bond-failure force (roughly 6 nN), the elastic modulus (about 28 nN), and also higher-order nonlinear elastic coefficients. These results show that nonlinear effects become important important even in the piconewton force range for synthetic polymers. By analogy, for DNA nonlinear effects should also be present and can explain the unexpected softening of DNA with respect to elongational stress as the salt concentration is decreased.[20]

Fluctuating Chain under Tension

As the starting point of our theory, we parametrize the chain such as to separate elongational degrees of freedom, described by the local backbone stretching $u(s)$, and bending degrees of freedom, characterized by the normalized tangent vector $\mathbf{t}(s)$ (such that $|\mathbf{t}(s)| = 1$), similarly to previous treatments.[5,15] The polymer configuration $\mathbf{r}(s)$ can be expressed as a function of the contour variable s of the unstretched polymer as

$$\mathbf{r}(s) = \int_{-\infty}^{s} \mathrm{d}s' \, [1 + u(s')]\mathbf{t}(s') \tag{1}$$

The partition function of a polymer parametrized in this fashion entails separate functional integrations over elongational and bending fluctuations (with the constraint $|\mathbf{t}(s)| = 1$ implicitly taken into account)

$$\mathcal{Z} = \int \mathcal{D}u \int \mathcal{D}\boldsymbol{t} \; \mathrm{e}^{-\mathscr{H}_0/k_\mathrm{B}T - \mathscr{H}_\mathrm{int}/k_\mathrm{B}T} \tag{2}$$

The energy of a polymer configuration is separated into a part which depends on the interaction v (in units of $k_\mathrm{B}T$) between polymer segments,

$$\mathscr{H}_\mathrm{int}/k_\mathrm{B}T = \int_{-\infty}^{\infty} \mathrm{d}s \int_{-\infty}^{s} \mathrm{d}s' \; \tau(s) \, \tau(s') v(|\mathbf{r}(s) - \mathbf{r}(s')|) \tag{3}$$

with $\tau(s)$ being the charge distribution along the polymer backbone for the case when $v(r)$ is the Coulomb interaction, and the bare part,

$$\mathscr{H}_0/k_\mathrm{B}T = \int_{-\infty}^{\infty} \mathrm{d}s \left\{ \frac{l_0}{2} \dot{\mathbf{t}}^2(s) + E[u(s)] - f \, [1 + u(s)] t_z(s) \right\} \tag{4}$$

which contains the elastic and the external force contributions. We restrict ourselves to infinitely long polymers and thus neglect end effects, which is a good approximation for strongly stretched polymers since the correlation length along the polymer is typically much smaller than the persistence length. The first term in eq 4 is the bending energy, with l_0 being the bare persistence length of the polymer, the second term describes the elastic elongational energy (in units of $k_\mathrm{B}T$), which we assume to be local, and the third term is due to the external stretching force f (in units of $k_\mathrm{B}T$), which we choose to act along the z-axis. In principle, there will also be a bare coupling between elongational and bending modes, which we do not consider in the present formulation of our theory. Also, twist degrees of freedom are neglected, which through their coupling to bending and elongational modes will also influence the response to an external force. However, as has been shown,[15] for DNA with freely rotating ends, the twist degrees can be integrated out and only lead to a renormalization of the stretching modulus at harmonic order. On the other hand, twist degrees of freedom are important for short DNA strands whose ends cannot rotate freely.[26] The elongational energy will in general also contain nonlocal terms, which arise due to the coupling of elongations of neighboring monomers. At a later stage, we take this nonlocality into account by using a discretized model with a lattice constant a which corresponds to the typical domain size of coupled monomers. In the case of ideal stretching behavior, one would have $E[u] = \gamma u^2/2$, characterized by a spring constant γ. Recent experiments indicate strongly nonlinear stretching energies.[13] It is therefore of interest to keep nonlinearities as well, and we indeed show that the strong-stretching limit can be calculated without specifying the elastic energy function $E[u]$ explicitly. Nonlinearities can be due to bond failure at very high forces, in which limit chemical bonds become softer. Other sources for nonlinearities are the coupling of bond angle distortion and bond length stretching for regular carbon polymer backbones or the more complicated structural transitions encountered with biopolymers such as DNA.

It is convenient to use an angular representation for the normalized tangent vector, $\mathbf{t} = (\sin\theta \sin\phi, \sin\theta \cos\phi, \cos\theta)$, since this representation obeys the constraint $|\mathbf{t}(s)| = 1$ automatically. The interaction energy eq 3 can now be systematically expanded in powers of the local elongation $u(s)$ and the angular derivatives $\dot{\theta}(s)$ and $\dot{\phi}(s)$ around the reference configuration of a straight rod. Up to second order we obtain

$$\frac{\mathscr{H}_\mathrm{int}}{k_\mathrm{B}T} = -g\int_{-\infty}^{\infty} \mathrm{d}s \; u(s) + \int_{-\infty}^{\infty} \mathrm{d}s \int_{-\infty}^{s} \mathrm{d}s' \, [u(s) \, u(s') G(s, s') + \dot{\theta}(s) \, \dot{\theta}(s') \, K(s,s')] \tag{5}$$

where we have omitted the constant energy contribution of the straight rod reference state. The azimuthal angle ϕ does not appear at this order. The constant g is given by (in units of $k_\mathrm{B}T$)

$$g = -\int_{-\infty}^{-0} \mathrm{d}w \int_{-\infty}^{+0} \mathrm{d}w' \; \tau(w) \, \tau(w') \, v'(w'-w) = -q^2 \sum_{j=1}^{\infty} j v'(ja) \tag{6}$$

and can be interpreted as an intrinsic force which pushes the monomers apart. The integration boundaries are set such as to avoid divergences from the interaction of one charge with itself. For electrostatic interactions, the stretching constant g diverges in the limit of a continuous charge distribution. We therefore have to use

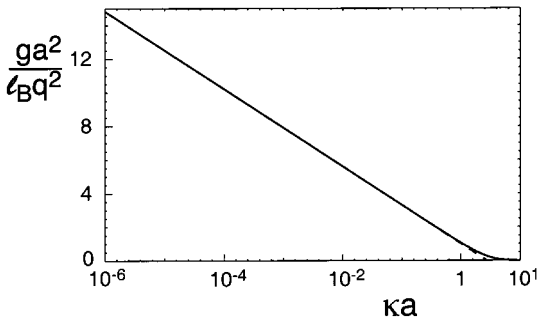

Figure 1. Rescaled linear electrostatic stretching force ga^2/l_Bq^2 as a function of the inverse screening length times monomer distance, κa (solid line). For $\kappa a < 1$, g is approximately given by $g \simeq l_Bq^2(\ln(1/\kappa a) + 1)/a^2$ (broken line).

a discrete charge distribution $\tau(s) = q\sum_i \delta(s - ai)$, where a denotes the distance between charges of valency q. In the following we will use the Debye−Hückel interaction $v(r) = l_B e^{-\kappa r}/r$, which takes the effect of salt screening into account on the linearized mean-field level. The Bjerrum length l_B is the length at which two unit charges interact with thermal energy, $l_B = e^2/(4\pi\epsilon k_BT)$; in water one typically has $l_B \approx 0.7$ nm. The screening length κ^{-1} is determined via $\kappa^2 = 8\pi l_B c_s$ and decreases as the salt concentration c_s increases. The sum in eq 6 can be done explicitly, and we obtain

$$g = \frac{l_B q^2}{a^2}\left(\kappa a \frac{e^{-\kappa a}}{1 - e^{-\kappa a}} - \ln(1 - e^{-\kappa a})\right) \qquad (7)$$

In Figure 1 we plot the rescaled linear electrostatic stretching force ga^2/l_Bq^2 as a function of the inverse screening length times monomer distance, κa (solid line). In most cases of practical interest, the screening length κ^{-1}will be larger than the distance between charges, such that $\kappa a < 1$, so that g is approximately given by $g \simeq l_Bq^2(\ln(1/\kappa a) + 1)/a^2$, which in Figure 1 is plotted as a broken line. The electrostatic stretching constant g thus diverges logarithmically in the limit of low salt concentration; since the prefactor is larger than unity for fully charged polyelectrolytes, the effect can be quite sizable, as we discuss now.

For a typical synthetic, fully charged polyelectrolyte (polysulfonated styrene or poly(acrylic acid)) one has $a = 0.25$ nm and $q = 1$; from eq 7 one obtains $g = 27$ nm^{-1} or $k_BTg = 111$ pN for $\kappa^{-1} = 1$ nm (or $c_s = 100$ mM for monovalent salt), $g = 53$ nm^{-1} or $k_BTg = 218$ pN for $\kappa^{-1} = 10$ nm (or $c_s = 1$ mM), and $g = 78$ nm^{-1} or $k_BTg = 325$ pN for $\kappa^{-1} = 100$ nm (or $c_s = 10$ μM). Note that g is measured in units of k_BT, so in order to get an estimate of the intrinsic force in units of newtons, we have to multiply by $k_BT = 4.14$ pN nm. The above results imply that rather large forces act on the backbone of fully charged polyelectrolytes. Clearly, the Debye−Hückel approach used in deriving eq 7 neglects nonlinear effects (counterion condensation[27,28]), which reduce the effective charge of the polymer. For low salt concentrations, the effective line charge density is reduced from q/a down to $1/l_B$, which corresponds to a decrease of the above calculated intrinsic forces by a factor of $^1/_9$. However, the situation is not so simple since at high salt concentrations the Debye−Hückel becomes exact (this happens when the surface potential is of the order of k_BT).[29] So one expects a crossover at high salt concentrations, where the above calculated forces are correct, to low salt concentrations, where the forces have to be multiplied by the counterion condensation correction factor of $^1/_9$.

For DNA, this intrinsic force might explain recent experiments, where it was found that the stretching-induced transition from the native B conformation to the overstretched S conformation shifts to lower forces as the salt concentration is decreased.[20] At salt concentrations of $c_s = 500$ mM this transition occurs at 65 pN, while at concentration of 50 mM (1 mM) it occurs at approximately 50 pN (30 pN). To see whether the force difference might be due to the repulsion between charges on the phosphate backbone, we use formula eq 7 with $a = 0.34$ nm and $q = 2$ to obtain the intrinsic stretching forces 126, 243, and 439 pN at salt concentrations 500, 50, and 1 mM, respectively. Clearly, the force differences are much larger than the experimentally measured ones. Using a renormalized charge of $q = {}^1/_2$, the intrinsic stretching forces turn out to be 8, 15.2, and 27.4 pN at salt concentrations 500, 50, and 1 mM, respectively. Now the differences between the intrinsic electrostatic stretching forces are of the same order as the differences between the experimentally measured forces at the transition. However, the same remarks about the breakdown of the simple counterion condensation argument at high salt concentrations from the last paragraph apply here as well. In essence, the intrinsic electrostatic stretching force g assists the external force f, an effect which will most easily be seen with structural transitions in biopolymers observed at moderate stretching forces such as the DNA-B−DNA-S transition.

The kernel of the quadratic stretching term in eq 5 reads

$$G(s,s') = \int_{-\infty}^{s} dw \int_{s'}^{-\infty} dw'\, \tau(w)\, \tau(w')\, v''(w'-w) \quad (8)$$

Since we assume the bare elastic energy E to be quite large, this quadratic contribution to the stretching energy is a small correction and will be neglected in the following.. The kernel of the bending term in eq 5, $K(s,s')$, has been derived by Barrat and Joanny.[19] Here we can assume the charge distribution along the polymer to be continuous, $\tau(s) = \tau_0 = q/a$, and the Fourier transformed kernel reads

$$\tilde{K}(p) = 2l_{OSF}\kappa^2 p^{-2}[(1 + \kappa^2 p^{-2})\ln(1 + \kappa^{-2}p^2) - 1] \quad (9)$$

In the zero-wavelength limit, one obtains $\tilde{K}(p\to 0) = l_{OSF}$, where $l_{OSF} = l_B\tau_0^2/4\kappa^2$ denotes the so-called Odijk−Skolnick−Fixman length.[16,17] At larger wavelengths, the kernel decays as $\tilde{K}(p) \simeq 4l_{OSF}\ln(p/\kappa)\kappa^2/p^2$, equivalent to a softening of the chain at small scales.

To insert the expansion of the interaction energy, eq 5, back into the partition function, eq 2, we have to express the angle-dependent part of eq 5 in terms of the Cartesian coordinates of the tangent vector, while satisfying $|\mathbf{t}(s)| = 1$. This is nontrivial, since eq 5 is an expansion in powers of the angles, while we need an expansion in powers of the tangent vector components. Progress can be made by first noting that the bending energy can be written in terms of the angular derivatives as $\dot{\mathbf{t}}^2 = \dot{\theta}^2 + \dot{\phi}^2 \sin^2\theta$. Up to quadratic order in $\mathbf{t}$ we obtain for the polar part $\dot{\theta}^2 \simeq \dot{t}_x^2 + \dot{t}_y^2 - (t_x\dot{t}_y - \dot{t}_xt_y)^2/(t_x^2 + t_y^2)$ and for the azimuthal part (which is of fourth order in the angles) $\dot{\phi}^2 \sin^2\theta \simeq (t_x\dot{t}_y - \dot{t}_xt_y)^2/(t_x^2 + t_y^2)$. The azimuthal contribution cancels part of the polar contribution. To second order in the tangent compo-

nents, the local bending energy can be written as $\dot{\mathbf{t}}^2 \simeq \dot{\mathbf{t}}_\perp^2$, where we introduce the perpendicular tangent vector $\dot{\mathbf{t}}_\perp^2 = \dot{t}_x^2 + \dot{t}_y^2$ and used the fact that $|\mathbf{t}| = 1$. By comparing the two expressions for the bending energy, it follows that the relation $\dot{\theta}^2 \simeq \dot{\mathbf{t}}^2$ holds up to second order in the tangent vector *and* the bending angles. We therefore in the following replace $\dot{\theta}^2$ by $\dot{\mathbf{t}}^2$ in eq 5.

Now we will perform the integral over the stretching amplitude $u(s)$. Since the stretching energy $E[u]$ is an arbitrary function, this cannot be done exactly in the general case. We therefore resort to a saddle-point approximation, treating elongational fluctuations (which turn out to be important in the presence of nonlinearities in the stretching energy $E[u]$) on the Gaussian level. Defining the inverse of the derivative of the elastic energy function as

$$H[E'[u]] = u \tag{10}$$

the saddle-point value of the elongational amplitude follows by minimization of the total energy $\mathscr{H}_{\text{int}} + \mathscr{H}_0$ as given by eqs 4 and 5 and reads

$$u_{\text{SP}}(s) = H[g + f t_z(s)]$$

Inserting this saddle-point elongation function into the Hamiltonian and expanding to quadratic order in deviations from this saddle point, $u(s) - u_{\text{SP}}(s)$, the Gaussian integrals over the elongational fluctuations can be performed. One obtains the partition function

$$\mathscr{Z} = \int \mathscr{D}\mathbf{t} \exp\left\{-\frac{1}{2}\int \mathrm{d}s\, \mathrm{d}s'\, \dot{\mathbf{t}}(s)\, \dot{\mathbf{t}}(s')[K(s-s') + l_0\delta(s-s')] + f\int \mathrm{d}s\, t_z(s)[1 + u_{\text{SP}}(s)] - \int \mathrm{d}s \left[E[u_{\text{SP}}(s)] - g u_{\text{SP}}(s) + \frac{1}{2a}\log\left(\frac{aE''[u_{\text{SP}}(s)]}{2\pi}\right)\right]\right\} \tag{11}$$

In this paper we are interested in the limit of strong stretching forces, which means that the polymer is aligned parallel to the z-axis and the magnitude of the perpendicular tangent vector is small. Expanding the Hamiltonian in powers of the perpendicular tangent vector $\mathbf{t}_\perp$ is therefore a good approximation, as we will discuss in more detail at the end of this paper. To quadratic order, one obtains the partition function

$$\mathscr{Z} = \int \mathscr{D}\mathbf{t} \exp\left\{-\frac{1}{2}\int \mathrm{d}s\, \mathrm{d}s'\, \dot{\mathbf{t}}(s)\, \dot{\mathbf{t}}(s')[K(s-s') + l_0\delta(s-s')] - \frac{\tilde{f}}{2}\int \mathrm{d}s\, \mathbf{t}_\perp^2\right\} \tag{12}$$

with the renormalized force

$$\tilde{f} = f\left(1 + H[g+f] + \frac{H''[g+f]}{2aH'[g+f]}\right) \tag{13}$$

In this expression, H' and H'' denote the first and second derivative of the function $H[x]$, respectively. As one can see, the electrostatic prestretching of the chain, expressed by the intrinsic force g, and the elongational fluctuations, regulated via the function H, enter into the effective force $\tilde{f}$ in a nonlinear fashion. The extension along the direction of the applied force, defined as $R_z = L_0\langle[1 + u(s)]t_z(s)\rangle$, where L_0 is the unperturbed length of the polymer (which is assumed to be large such that end effects are negligible), follows to quadratic order in $\mathbf{t}_\perp$ as

$$\frac{R_z}{L_0} = 1 + H[g+f] - \frac{1}{2}(1 + H[g+f] + fH'[g+f])\langle \mathbf{t}_\perp^2\rangle \tag{14}$$

The force renormalization, eq 13, and the result for the total chain extension, eq 14, constitute the main results of this part. By explicitly integrating out the elongational fluctuations, we obtain coupling terms in the stretching response of the chain which had been neglected in previous treatments[5,15] but which can play an important role, as will be discussed in detail later on.

The expectation value of the perpendicular tangent vector components in eq 14 is given by

$$\langle \mathbf{t}_\perp^2\rangle = \int_{-\infty}^{\infty} \frac{\mathrm{d}p/\pi}{\tilde{f} + p^2[l_0 + \tilde{K}(p)]} \tag{15}$$

As has been shown by Barrat and Joanny, the electrostatic persistence length is scale dependent, being given by l_{OSF} on scales larger than the screening length κ^{-1} and decreasing rapidly for smaller scales.[19] For a semiflexible chain with bare persistence length l_0 under tension force $\tilde{f}$, the deflection length, i.e., the typical scale of bending fluctuations,[30] is $\lambda \sim \sqrt{l_0/\tilde{f}}$ and thus becomes smaller as the force increases. The softening of the chain due to the scale dependence of the electrostatic persistence should be noticeable for $\lambda < \kappa^{-1}$ or $\tilde{f} > l_0\kappa^2$; it is thus expected that the chain becomes softer as the pulling force increases.[6] Indeed, for large forces $\tilde{f} \gg l_0\kappa^2$ the integral eq 15 gives $\langle \mathbf{t}_\perp^2\rangle \simeq 1/\sqrt{\tilde{f}l_0}$, while for small forces $\tilde{f} \ll l_0\kappa^2$ one finds $\langle \mathbf{t}_\perp^2\rangle \simeq 1/\sqrt{\tilde{f}(l_0 + l_{\text{OSF}})}$. This suggests the definition of an effective persistence length l_{eff} as

$$\langle \mathbf{t}_\perp^2\rangle = (\tilde{f}l_{\text{eff}})^{-1/2} \tag{16}$$

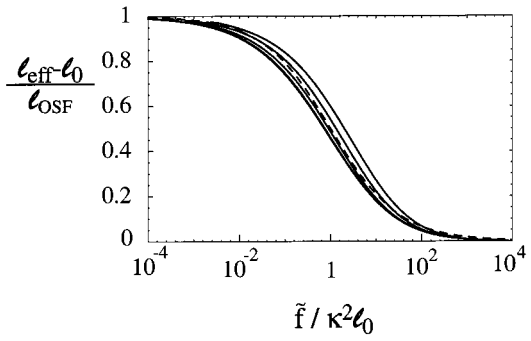

Figure 2. Effective rescaled persistence length $(l_{\text{eff}} - l_0)/l_{\text{OSF}}$ as a function of the rescaled force $\tilde{f}/l_0\kappa^2$ for five different values of the ratio of the electrostatic persistence l_{OSF} and the bare persistence length l_0, $l_{\text{OSF}}/l_0 = 0.1$, 1, 10, 100, 1000 (solid lines, from bottom to top). Note that the curves for $l_{\text{OSF}}/l_0 = 0.1$ and 1 are indistinguishable on this scale. The broken line denotes the heuristic scaling function described in the text.

In Figure 2 we plot the rescaled effective persistence length $(l_{\text{eff}} - l_0)/l_{\text{OSF}}$ as determined by eqs 15 and 16 as a function of the rescaled force $\tilde{f}/l_0\kappa^2$ for five different ratios of the electrostatic persistence length l_{OSF} and the bare persistence length l_0 (solid lines). It is seen that

all five curves are rather similar and are in fact well described by the heuristic expression

$$\frac{l_{\text{eff}} - l_0}{l_{\text{OSF}}} = \frac{1}{1 + (\tilde{f}/l_0\kappa^2)^{0.58}} \tag{17}$$

which is shown as a broken line. It is thus demonstrated that the effective persistence length l_{eff} can be described by a universal scaling function over 5 orders of magnitude of the ratio l_{OSF}/l_0. Quite remarkably, the crossover occurs over 4 orders of magnitude of the applied force, which has profound consequences for the interpretation of stretching experiments of DNA and synthetic polyelectrolytes, as we discuss now. The crossover occurs at a force $f^* = l_0\kappa^2$. For DNA with a bare persistence length $l_0 \approx 30$ nm[21] at physiological salt concentration $c_s = 100$ mM (corresponding to a screening length $\kappa^{-1} \approx 1$ nm) we obtain $f^* k_B T = 120$ pN, which is larger than the forces probed in the magnetic bead experiments.[2] Indeed, the experimental results can be fitted by an effective persistence length roughly given by the sum of the bare and electrostatic persistence lengths.[6] For low salt concentrations, $c_s = 1$ mM (corresponding to a screening length $\kappa^{-1} \approx 10$ nm), we obtain a crossover force $f^* k_B T = 1.2$ pN, well inside the experimentally accessible force region.[2] Here the results cannot be fitted with a single effective persistence length.[6] For synthetic polyelectrolytes with $l_0 \approx 1$ nm we obtain $f^* k_B T = 4$ pN for $c_s = 100$ mM and $f^* k_B T = 40fN$ for $c_s = 1$ mM. Indeed, extension curves for synthetic charged polymers at forces typically measurable with the AFM can be very well fitted by the bare persistence length.[12,13] Clearly, a reanalysis of experimental data with the crossover function eq 17 might yield better fits and more reliable estimates for the bare persistence length l_0.

The above discussion might suggest that, since the crossover force decreases with decreasing salt concentration, the chain becomes more flexible as the screening length increases (which would be counterintuitive, to say the least). This is clearly not so, which one can see from the first-order correction to the expectation value $\langle \mathbf{t}_\perp{}^2 \rangle$ for large forces $\tilde{f}/l_0\kappa^2 \gg 1$, which follows from eq 15 and reads

$$\langle \mathbf{t}_\perp{}^2 \rangle \simeq \frac{1}{(\tilde{f} l_0)^{1/2}} \left[1 - \frac{\kappa^2 l_{\text{OSF}}}{\tilde{f}} \ln\left(\frac{\tilde{f}}{l_0\kappa^2} \right) \right]$$

Clearly, for decreasing salt concentration (decreasing κ), since the factor $\kappa^2 l_{\text{OSF}} = l_B \tau_0{}^2/4$ is independent of κ, the value of $\langle \mathbf{t}_\perp{}^2 \rangle$ decreases; the chain becomes effectively stiffer, as one would expect. Note, however, that the dependence on the salt concentration is logarithmic and thus very weak.

Ab Initio Calculation for Polymer Elasticity

In the calculations of the last section the elastic properties of the polymer chain were shown to influence the stretching properties considerably. The simplest model for the stretching energy of a polymer is the ideal spring model,

$$E[u] = \gamma u^2/2 \tag{18}$$

where all but the linear elastic response is neglected and which leads to the inverse function $H[x] = x/\gamma$ and the first derivative $H'[x] = 1/\gamma$. Note that the effect of elongational fluctuations (proportional to H''/H' in eq 13) in this ideal case cancels out since $H''[x] = 0$. The stretching response determined by eqs 13 and 14 for the linear elasticity case reads

$$\frac{R_z}{L_0} = 1 + \frac{g+f}{\gamma} - \frac{1 + (g+2f)/\gamma}{2\sqrt{l_{\text{eff}} f (1 + (g+f)/\gamma)}} \tag{19}$$

and thus differs considerably from previous expressions.[5,15] The coupling between bending fluctuations and the elongational response, embodied by the γ-dependent terms in the third term in eq 19, will be important for polymers which are rather soft with respect to elongational deformations.

In principle, the full nonlinear elasticty function $H[x]$ could be determined from a global fit of the extension curve eq 14 to experimental data. It can also be calculated using ab initio quantum-chemical methods, as has recently been done for poly(ethylene glycol) chains[31] and for short oligomers of different chemical constitution.[32] In this section we complement our perturbative calculations with quantum-chemistry ab initio calculations using the GAMESS package.[33] We start with our results for very short polymers, namely propane molecules consisting of three carbon atoms. In Figure 3a we show the binding energy per C−C bond in units of $k_B T$ using three different basis sets, namely Slater-type orbitals with six Gaussians (STO-6G), shown

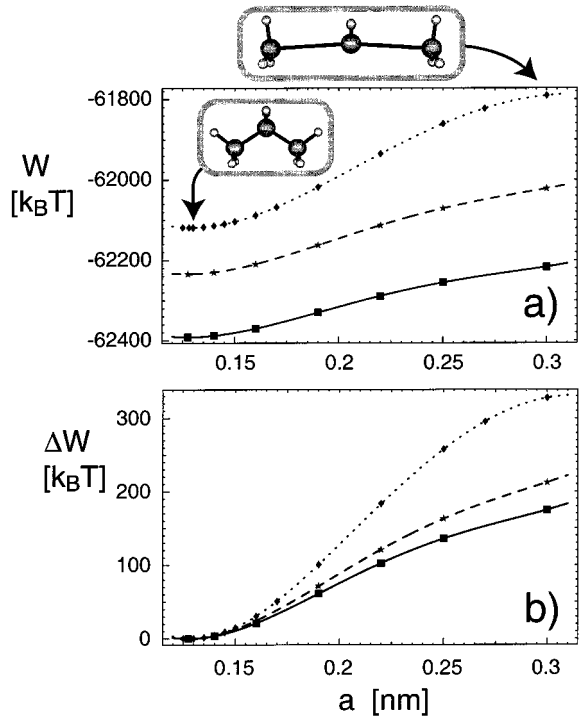

Figure 3. Ab initio quantum-chemistry results for the total binding energy per C−C bond in units of $k_B T$ for a propane molecule as a function of the projected bond length a. In (a) we show the results for three different basis sets, namely Slater-type orbitals with six Gaussians (STO-6G), shown as diamonds and fitted by a dotted line, triple-ζ-valence (TZV) functions, shown as stars and fitted by a broken line, and finally the second-order Moller−Plesset perturbation theory results (TZV-MP2), shown as squares and fitted by a solid line. All calculations were performed using the unrestricted Hartree−Fock method (UHF). The configurations shown were obtained at projected bond length $a = 0.13$ nm and $a = 0.3$ nm. In (b) we show the energy per bond where we have subtracted from each curve the energy at the equilibrium bond length.

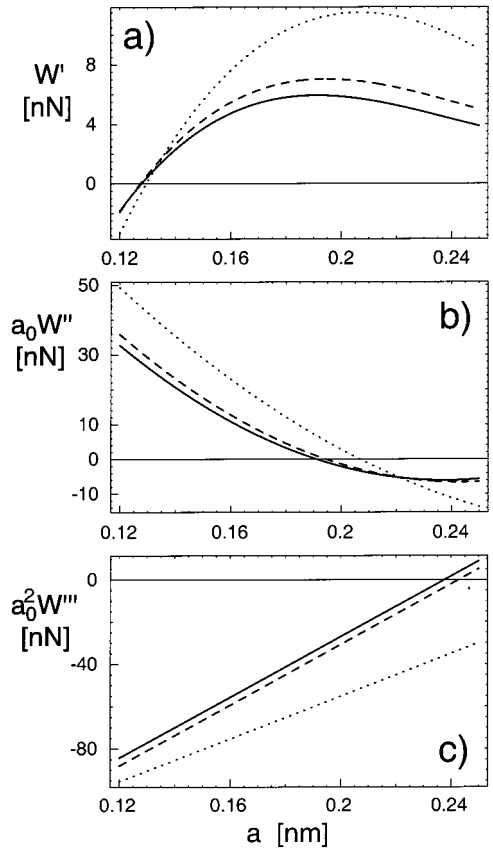

Figure 4. Shown are the first, the second, and the third derivative of the energy shown in Figure 3 using the same notation. The force curves in (a) exhibit an instability at a bond length of roughly $a \approx 0.2$ nm. The TZV-MP2 calculation (solid line) gives a force threshold of 6 nN. The second derivative shown in (b) determines the stretching modulus, which at equilibrium is of the order of 28 nN (based on the TZV-MP2 result, solid line).

as diamonds and fitted by a dotted line, triple-ζ valence (TZV) functions, shown as stars and fitted by a broken line, and finally the second-order Moller−Plesset perturbation theory results (TZV-MP2), shown as squares and fitted by a solid line. All calculations were performed using the unrestricted Hartree−Fock method (UHF). As one can see, the better the basis set, the lower the binding energy. The different calculations allow to estimate roughly the error one is making in choosing a necessarily incomplete basis set. In Figure 3a we also show two configurations obtained at projected bond length $a = 0.13$ nm and $a = 0.3$ nm. As one can see, the molecular response to the external stretching force consists both of bond angle deformation and bond stretching. The minimal energies occur for projected bond lengths of $a_0 = 0.1295$ nm (UHF-STO-6G), $a_0 = 0.1274$ nm (UHF-TZV), and $a_0 = 0.1278$ nm (UHF-TZV-MP2). The fits were done using a fourth-order polynomial. To appreciate better the stretching response, we show in Figure 3b the energy per bond where we have subtracted from each curve the energy at the equilibrium bond length. As one can, the STO-6G calculation greatly overestimates the energy increase upon stretching, the TZV basis set performs much better since the wave function is more delocalized and polarization effects, which are important close to bond failure, can be taken into account. The additional effects of correlations, as embodied in the MP2 calculation, though important for the absolute binding energies, are not so important for the stretching energy, as demonstrated in Figure 3b. In Figure 4a we show the stretching force, obtained by taking a derivative of the polynomial fit function. In agreement with earlier results,[32] the force curves exhibit an instability at a bond length of roughly $a \approx 0.2$ nm. Our best estimate, based on the TZV-MP2 calculation (solid line), gives a force threshold of 6 nN, which is close to the estimate of ref 32 obtained using density functional theory. The second derivative shown in Figure 4b determines the stretching modulus, which at equilibrium is of the order of 28 nN (based on the TZV-MP2 result, solid line). Not surprisingly, the bonds become weaker upon stretching and at bond failure, the stretching modulus is zero. Finally, in Figure 4c we show the third derivative of the stretching energy, which plays a certain role when estimating the role of bond elongational fluctuations on the stretching response upon force, as will be discussed shortly.

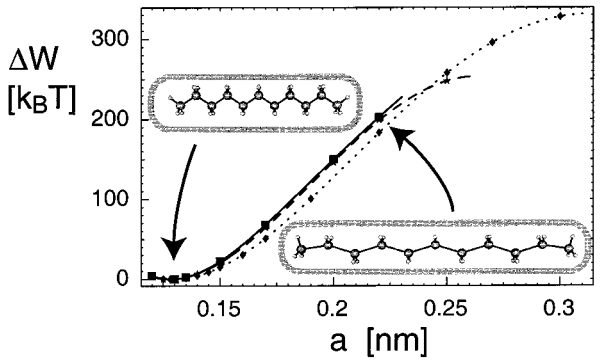

Figure 5. Total binding energies per C−C bond are shown for alkanes consisting of 7 (stars, fitted by a broken line) and of 11 (squares, solid line) carbon atoms in comparison with the data for propane (diamonds, dotted line). All calculations are performed using the STO-6G basis set. The rather small differences show that ab initio calculations for small molecules give rather good estimates for polymers.

To estimate the effect of increasing molecular length, we in Figure 5 show calculations for alkanes consisting of 7 (stars, fitted by a broken line) and of 11 (squares, solid line) carbon atoms in comparison withe the data for propane (diamonds, dotted line). All calculations are performed using the STO-6G basis set. As one can see, the effects of increasing length are rather small; in fact, the data for 7 and 11 carbon atoms almost coincide. This shows that cooperative effects on the quantum level are negligible when stretching is considered. For higher stretching forces, the optimized moleculecular structures of the alkane chains comprising 7 and 11 carbon atoms exhibit some type of reconstruction; i.e., the molecule can minimze the total energy by choosing a molecular structure where the carbon−carbon bond lengths vary along the chain. This is not surprising, since the total bond energy of a long chain under tension is typically minimized by a broken configuration long before the instability limit of a single bond is reached. The reconstruction can be understood as a collective soft-mode precursor for bond breakage.

To establish the connection with our perturbational results in the last section, we need to calculate the inverse function $H(x)$ defined in eq 10. To accomplish this, we consider the nonlinear elastic energy function

$$E(u) = \frac{\gamma}{2} u^2 - \frac{\delta}{6} u^3 \qquad (20)$$

The values of the coefficients can be directly read of from

Figure 4 and are given by $\gamma k_B T = 28$ nN and $\delta k_B T = 80$ nN or, in rescaled units, $\gamma = 7\ \mathrm{nm}^{-1}$ and $\delta = 19\ \mathrm{nm}^{-1}$. The inverse function follows as

$$H(x) = \frac{\gamma}{\delta} - \sqrt{\frac{\gamma^2}{\delta^2} - \frac{2x}{\delta}} \tag{21}$$

and the various derivatives of it featured in the expressions eqs 13 and 14 are

$$H'(x) = \frac{1}{\delta\sqrt{\frac{\gamma^2}{\delta^2} - \frac{2x}{\delta}}} \tag{22}$$

and

$$\frac{H''(x)}{H'(x)} = \frac{1}{\delta\left(\frac{\gamma^2}{\delta^2} - \frac{2x}{\delta}\right)} \tag{23}$$

The main point here is that as the bond instability (defined by $E''[u] = 0$ or $H'[x] = \infty$, leading to the critical bond length $u^* = \gamma/\delta$) is approached, the correction terms present in eqs 13 and 14 become large. For small effective forces $g + f$ (which contains both the external force f and the intrinsic force g), the function $H[x]$ behaves as $H[x] \simeq x/\gamma$ and the term $H[g + f]$ in eq 14 gives the standard linear-response result $H[g + f] \simeq (g + f)/\gamma$. However, as the intrinsic or the external force grows, nonlinearities lead to a larger response to the force; as can be seen from the divergence of the first derivative eq 22, the bonds are effectively softer. Since the intrinsic force increases as the salt concentration is decreased, one expects the elastic modulus to go down for lower salt concentrations.

Similar effects are expected for DNA, which exhibits an overstretching transition at a force of roughly 60 pN for large salt concentrations. The simplest elastic energy function to describe this behavior contains two competing local minima.[15] By analogy with our arguments for synthetic polymers above, nonlinear effects will decrease the elastic modulus as the effective force (including the external and the intrinsic force) is increased, which explains the observed softening of DNA as the salt concentration is decreased.[20]

Discussion

First, we would like to comment on when the restriction to aligned chains, equivalent to the Gaussian approximation for the fluctuations of $\mathbf{t}_\perp$, an approximation used throughout this paper, is valid and when the neglect of self-avoidance, which was recently investigated using self-consistent methods,[34] becomes questionable. To that end, it is useful to consider the scaling of an unstretched polyelectrolyte first. The end-to-end radius R of a strongly charged polyelectrolyte chain shows three distinct scaling ranges. For a chain length L smaller than the total persistence length l, which is the sum of the bare and electrostatic persistence lengths, $l = l_0 + l_{OSF}$, the end-to-end radius grows linearly with the length, $R \sim L$. The second virial coefficient of a rod of length l and diameter d is $v_2 \sim l^2 d$. The standard Flory treatment for a semiflexible chain then gives a swollen radius $R \sim (v_2 L^3/l)^{1/5}$. This radius is only realized above a minimal chain length $L > L^* \sim l^7/v_2^2 \sim l^3/d^2$. For elongated segments with $l \gg d$, or, equivalently, for a highly charged polyelectrolyte, we therefore have an intermediate range of chain lengths $l < L < L^*$ for which the chain is predicted to be Gaussian. This is clearly different in two dimensions, where the second virial coefficient is $v_2 \sim l^2$ and the intermediate Gaussian regime consequently vanishes, which is consistent with experiments on adsorbed DNA polymers.[35] For charged chains, the effective width d is for small salt concentrations given by the screening length; i.e., one has in this case $d \sim \kappa^{-1}$ plus logarithmic corrections. As was shown by Pincus,[36] the force (in units of $k_B T$) is related to the stretching blob size ξ by $f \sim 1/\xi$. The crossover from the strong-stretching regime, where the polymer is totally stretched out, and the weak-stretching regime, where the polymer forms blobs,[37] occurs when the stretching-blob size ξ is of the order of the total persistence length or when $f^{**} \sim 1/l$. For DNA with a total persistence length $l \simeq 50$ nm at physiological salt concentrations, we obtain $f^{**} k_B T \simeq 100fN$. This force is typically much smaller than the crossover force f^* calculated before, at least for not too low salt concentrations. We therefore have a separation of crossover forces, opening up an intermediate force range $f^{**} < f < f^*$ where the DNA is electrostatically stiffened but not yet coiling up. For a synthetic polymer with $l \simeq 1$ nm we obtain $f^{**} k_B T \simeq 4$ pN, which is of the same order as f^*. The softening of the electrostatic persistence length derived above occurs at the same force range where the polymers start to coil up, which calls for a more refined approach in the low-force region. The crossover force to the regime where self-avoidance becomes important is $f^{***} \sim 1/\xi$ with ξ given by the size of a chain with threshold length L^*, i.e., $\xi \sim (lL^*)^{1/2}$.[36] The crossover force follows as $f^{***} \sim d/l^2 \sim (d/l) f^{**}$. The last equation shows that self-avoidance becomes important for much lower forces than where the polymer forms coils, at least for highly elongated segments. The complete scaling description of the elastic response of a polyelectrolyte can be sketched as follows: For $f < f^{***}$ self-avoidance is important, and the extension goes as $R_z \sim L f^{2/3} (ld)^{1/3}$. For $f^{***} < f < f^{**}$ self-avoidance is irrelevant, and we have $R_z \sim Lfl$; the chain behaves like an ideal Gaussian spring consisting of many random coils. Finally, for $f^{**} < f$ the chain is almost completely flattened out, and the Gaussian approximation for the perpendicular tangent vector components employed in this paper is valid. The extension is dominated by bending fluctuations and given by eqs 14 and 16. For $f < f^*$ the effective persistence length is given by the sum of bare and electrostatic persistence length, while for $f > f^*$ the electrostatic contribution to the persistence gradually fades away, as determined by the scaling function shown in Figure 2. Our calculations are done on the Debye−Hückel level which neglects nonlinear electrostatic effects as present within the Poisson−Boltzmann approach.[27,28] The counterion condensation theory in its simplest formulation consists of replacing the bare line charge density $\tau_0 = q/a$ by the renormalized line-charge density $\tau_0 = 1/l_B$. As has been shown by Fixman numerically, this approach is only valid at low salt concentrations; the Debye−Hückel approach becomes valid at sufficiently high salt concentrations even for highly charged polymers.[29]

Finally, our arguments for the shift of the B-DNA−S-DNA transition are purely phenomenological in the sense that we simply calculate the intrinsic stretching force due to electrostatic repulsions within the molecule,

which is additive to any externally applied force. Our arguments do not depend on the mechanism of the B-DNA−S-DNA transition, for which more detailed microscopic information is needed[38] and which has been considered in a number of previous theories.[22,39] Likewise, it is for our arguments rather unimportant whether the B-DNA−S-DNA transition is accompanied by the denaturation transition where the two DNA strands separate from each other, as has been suggested recently.[25] An argument supporting the belief that the B-DNA−S-DNA and the melting transitions are (at least in principle) two distinct transitions is furnished by pulling experiments on double-stranded poly(dG-dC) DNA, where the B-DNA−S-DNA transition occurs at 65 pN while the melting transition is raised to 300 pN because of the higher base-pairing free energy.[8,24] For typical DNA with a nonperiodic distribution of A−T and G−C base pairs, the forces needed to induce the two transition are closer and even might coalesce, depending on the respective fractions of A−T and G−C base pairs.

In summary, by formulating a theory incorporating elongational and bending fluctuations on the same footing while treating the intrachain electrostatic repulsions on a perturbative level, we presented the stretching response of a charged, semiflexible and extensible chain in the strong-force limit. The electrostatic repulsion within the chain leads to an intrinsic force, which tends to push the monomers apart and which has measurable effects in the case of a configurational force-induced transition (as for example the B-DNA−S-DNA transition[20]). Nonlinear effects typically tend to make polymers softer with respect to elongations as the stretching increases, as we demonstrated explicitly for simple synthetic polymer using ab initio methods. For DNA this effect explains the elongational softening observed as the salt concentration is decreased,[20] since the intrinsic electrostatic force increases with lower salt concentrations. Finally, the scale or force-dependent electrostatic persistence length can be described by a universal scaling function, which should make fits to experimental data quite easy.

Acknowledgment. Useful discussions with M. Grosholz, T. Hugel, H. Clausen-Schaumann, A. Pfau, M. Seitz, and H. E. Gaub are gratefully acknowledged.

References and Notes

(1) Clausen-Schaumann, H.; Seitz, M.; Krautbauer, R.; Gaub, H. E. *Curr. Opin. Chem. Biol.* **2000**, *4*, 524.
(2) Smith, S. B.; Finzi, L.; Bustamente, C. *Science* **1992**, *258*, 1122.
(3) Bustamente, C.; Marko, J. F.; Siggia, E. D. *Science* **1994**, *265*, 1600.
(4) Vogolodskii, A. *Macromolecules* **1994**, *27*, 5623.
(5) Odijk, T. *Macromolecules* **1995**, *28*, 7016.
(6) Marko, J. F.; Siggia, E. D. *Macromolecules* **1995**, *28*, 8759.
(7) Ha, B. Y.; Thirumalai, D. *J. Chem. Phys.* **1997**, *106*, 4243.
(8) Rief, M.; Clausen-Schaumann, H.; Gaub, H. E. *Nature Struct. Biol.* **1999**, *6*, 346.
(9) Rief, M.; Gautel, M.; Oesterhelt, F.; Fernandez, J. M.; Gaub, H. E. *Science* **1997**, *276*, 1109.
(10) Rief, M.; Oesterhelt, F.; Heymann, B.; Gaub, H. E. *Science* **1997**, *275*, 1295.
(11) Oesterhelt, F.; Rief, M.; Gaub, H. E. *New J. Phys.* **1999**, *1*, 6.
(12) Ortiz, C.; Hadziioannou, G. *Macromolecules* **1999**, *32*, 780.
(13) Hugel, T.; Grosholz, M.; Clausen-Schaumann, H.; Pfau, A.; Gaub, H.; Seitz, M. *Macromolecules* **2001**, *34*, 1039.
(14) Evans, E.; Ritchie, K.; Merkel, R. *Biophys. J.* **1995**, *68*, 2580.
(15) Marko, J. F. *Phys. Rev. E* **1998**, *57*, 2134.
(16) Odijk, T. *J. Polym. Sci.* **1977**, *15*, 477.
(17) Skolnick, J.; Fixman, M. *Macromolecules* **1977**, *10*, 944.
(18) Netz, R. R.; Orland, H. *Eur. Phys. J. B* **1999**, *8*, 81.
(19) Barrat, J.-L.; Joanny, J.-F. *Europhys. Lett.* **1993**, *24*, 333.
(20) Baumann, C. G.; Smith, S. B.; Bloomfield, V. A.; Bustamente, C. *Proc. Natl. Acad. Sci. U.S.A.* **1997**, *94*, 6185.
(21) Borochov, N.; Eisenberg, H.; Kam, Z. *Biopolymers* **1981**, *20*, 231.
(22) Cluzel, P.; Lebrun, A.; Heller, C.; Lavery, R.; Viovy, J. L.; Chatenay, D.; Caron, F. *Science* **1996**, *271*, 792.
(23) Smith, S. B.; Cui, Y.; Bustamente, C. *Science* **1996**, *271*, 795.
(24) Clausen-Schaumann, H.; Rief, M.; Tolksdorf, C.; Gaub, H. E. *Biophys. J.* **2000**, *78*, 1997.
(25) Williams, M. C.; Wenner, J. R.; Rouzina, I.; Bloomfield, V. A. *Biophys. J.* **2001**, *80*, 874; **2001**, *80*, 1932.
(26) Strick, T. R.; Allemand, J. F.; Bensimon, D. *Science* **1996**, *271*, 1835.
(27) Manning, G. S. *J. Chem. Phys.* **1969**, *51*, 924.
(28) Manning, G. S. *Q. Rev. Biophys.* **1978**, *11*, 179.
(29) Fixman, M. *J. Chem. Phys.* **1982**, *76*, 6346.
(30) Odijk, T. *Macromolecules*, **1983**, *16*, 1340; **1984**, *17*, 502.
(31) Kreuzer, H. J.; Wang, R. L. C.; Grunze, M. *New J. Phys.* **1999**, *1*, 1.21.
(32) Beyer, M. K. *J. Chem. Phys.* **2000**, *112*, 7307.
(33) Schmidt, M. W.; Baldrige, K. K.; Boatz, J. A.; Elbert, S. T.; Gordon, M. S.; Jensen, J. J.; Koseki, S.; Matsunaga, N.; Nguyen, K. A.; Su, S.; Windus, T. L.; Dupuis, M.; Montgomery, J. A. *J. Comput. Chem.* **1993**, *14*, 1347.
(34) Lee, N.; Thirumalai, D. *Eur. Phys. J. B* **1999**, *12*, 599.
(35) Maier, B.; Rädler, J. O. *Macromolecules* **2000**, *33*, 7185.
(36) Pincus, F. *Macromolecules* **1976**, *9*, 386.
(37) Chatellier, X.; Senden, T. J.; Joanny, J. F.; di Meggio, J. M. *Europhys. Lett.* **1998**, *41*, 303.
(38) Kosikov, K. M.; Gorin, A. A.; Zhurkin, V. B.; Olson, W. K. *J. Mol. Biol.* **1999**, *289*, 1301.
(39) Ahsan, A.; Rudnick, J.; Bruinsma, R. *Biophys. J.* **1998**, *74*, 132.

MA010555U